

Article

Microporous Zeolites as Catalysts for the Preparation of Decyl Glucoside from Glucose with 1-Decanol by Direct Glucosidation

Kyong-Hwan Chung¹, Hyunwoong Park², Ki-Joon Jeon³, Young-Kwon Park⁴
and Sang-Chul Jung^{1,*}

¹ Department of Environmental Engineering, Suncheon National University, 315 Maegok-Dong, Suncheon 540-742, Jeonnam, Korea; likeu21@naver.com

² School of Energy Engineering, Kyungpook National University, Daegu 702-701, Korea; hwp@knu.ac.kr

³ Department of Environmental Engineering, Inha University, 100 Inha-ro, Nam-gu, Incheon 402-751, Korea; Kjjeon@inha.ac.kr

⁴ School of Environmental Engineering, University of Seoul, 163 Seoulsiripdaero, Dongdaemun-gu, Seoul 130-743, Korea; catalica@uos.ac.kr

* Correspondence: jcs@suncheon.ac.kr; Tel.: +82-61-750-3814

Academic Editors: Shaobin Wang and Xiaoguang Duan

Received: 10 November 2016; Accepted: 15 December 2016; Published: 21 December 2016

Abstract: The catalytic properties of microporous zeolite catalysts were evaluated in the synthesis of decyl glucoside from glucose with 1-decanol by direct glucosidation. The effects of the acidic properties and pore structure of the zeolite catalysts on the glucose conversions and decyl glucoside yields were investigated. The conversions of glucose on the H⁺ ion-exchanged FAU, MFI, and BEA zeolite catalysts were above 70%. The conversion increased with decreasing acid strength of the catalysts. The highest conversion and yield of decyl glucoside were exhibited on the H-FAU(3) zeolite catalyst. The catalytic activities were enhanced with increasing amounts of acid sites. The selectivity of decyl glucopyranoside increased with decreasing Si/Al values for the same zeolite catalysts. The pore structure of H-FAU zeolite would allow sufficient spatial restriction to produce decyl glucopyranoside through the isomerization of decyl glucofuranoside into decyl glucopyranoside in its extensive pore channels. The selectivities of the decyl glucoside isomers relied significantly on the restricted transition state to the primary products due to their pore topologies.

Keywords: decyl glucoside; zeolite catalysts; direct glucosidation; selectivity; alternative surfactant

1. Introduction

Alkyl phenol ethoxylates and linear alkylbenzene sulfonates have been used as major surfactants. They degrade in the aerobic conditions found in sewage treatment plants and in the metabolite, nonylphenol, which has been found to be an endocrine disruptor [1]. Concerns have been expressed about alkylphenols owing to their environmental prevalence and their potential effect as xenoestrogen and endocrine disruptors [2,3]. Nonylphenol has been reported to have estrogenic activity based on its proliferation induction and up-regulation of progesterone receptor I human estrogen-sensitive breast tumor cells [4]. It has been established recently that nonylphenol has antiandrogenic activity, which means that it affects the appropriate functioning of the androgens that are necessary for the normal growth and reproductive organs of males [5].

Long-chain alkyl glucosides have excellent surfactant properties with biodegradability and low toxicity [6,7]. Therefore, they have recently been considered as alternative surfactants to alkylphenols [8]. Alkyl glucosides as the industrially manufactured products are widely known. The preparation of the alkyl glucosides by the Fischer method, which involved the reaction of glucose with hydrophilic

alcohols was applied to hydrophobic alcohols with alkyl chains from octyl (C₈) up to hexadecyl (C₁₆) alcohols [9]. They have been used as food emulsifiers, cosmetic surfactants, and pharmaceutical dispersing agents [10,11]. They produce vesicular microaggregates and micellar. Their properties are dependent on the shape and length of the hydrocarbon tail driven by the fine balance between their hydrophilic and hydrophobic interactions [12].

Decyl glucoside, as a long-chain alkyl glucoside, has been applied in cosmetic formularies as a mild non-ionic surfactant. This cleanser is used by personal care companies since it is biodegradable and gentle for all hair types. Decyl glucoside is prepared by the reaction of glucose obtained from cornstarch with decanol, which is derived from coconut. Studies concerning the use of decyl glucose in antiseptic, sunscreen, and hair products are described in some of the published literature [13–18]. It has been adopted various acid catalysts and additives such as furandicarboxylic acid and sulfoxides in preparation of alkyl polyglycosides [19,20].

The alkyl glucosides obtained from monohydric alcohols can be synthesized by the Fischer reaction [21,22]. However, they are prepared through a two-step process, because the solubility of glucose in long-chain fatty alcohols is quite low. In the first process, short-chain alkyl glucosides are formed from the glucosidation of short-chain fatty alcohols. The first products are soluble in fatty alcohols. Finally, in the second stage, long-chain alkyl glucosides are prepared by the transacetalation of the initial products [23]. In preparation of dodecyl glucoside, the direct glucosidation reaction was attempted in order to compare this route with the two-step glucosidation reaction [24]. However, this method requires a complicated pre-treatment and the further supply of reactant during the reaction. Moreover, the heating of the reactants under vacuum is required prior to the reaction. Moreover, the system needs a further supply of glucose at regular intervals to enhance the solubility of glucose in the alcohols.

In this study, the synthesis of decyl glucosides is attempted using single-step direct glucosidation over microporous zeolite catalysts. We describe a single-step direct glucosidation reaction without any complicated processes during the reaction. The catalytic activities of the zeolites, having various acid strengths and pore topologies, were estimated in relation to the conversion and yields of the decyl glucoside isomers. The effects of the acidities and pore topologies of the zeolite catalysts were investigated in the glucosidation reaction.

2. Results and Discussion

2.1. Physicochemical Properties of the Zeolite Catalysts

The X-ray diffraction (XRD) patterns of the zeolites were in good agreement with those published in the literature [25]. The results indicate that the zeolites were highly crystalline. The crystal sizes estimated from the SEM images of the MFI and FAU zeolites were about 0.5 μm and that of the MOR zeolite was 1.5–2.0 μm . Figure 1 presents the N₂ physisorption isotherms of the zeolites (FAU, MOR, MFI) were typical Langmuir isotherms, whereas that of the BEA zeolite showed an increase in P/P_0 to 0.4–0.9. The large adsorptions of nitrogen on the FAU and BEA zeolites were caused by their large pore volumes and void fractions. The pore volumes and surface areas of the zeolites according to the Si/Al values are listed in Table 1. The cage volume of FAU calculated using Marler's equation [26] was 1150 \AA^3 , and is dependent on its framework.

The acidities of the zeolites differed considerably according to their framework, as shown in Figure 2. The NH₃-temperature programmed desorption (NH₃-TPD) profiles can be estimated as the summation of the curves of the *h*-peak and *l*-peak [27,28]. The peak maximum of the *h*-peak, which corresponded to the strong acid sites, was obtained at around 350–550 $^{\circ}\text{C}$, while that of the *l*-peak appeared at about 250 $^{\circ}\text{C}$, which indicates that it corresponded to the weak acid sites [27]. The large *h*-peak of the MOR zeolite was due to its numerous strong acid sites. Even though the BEA zeolite has an MR of 12 as the MOR zeolite does, it had a larger *l*-peak owing to its weak acidity.

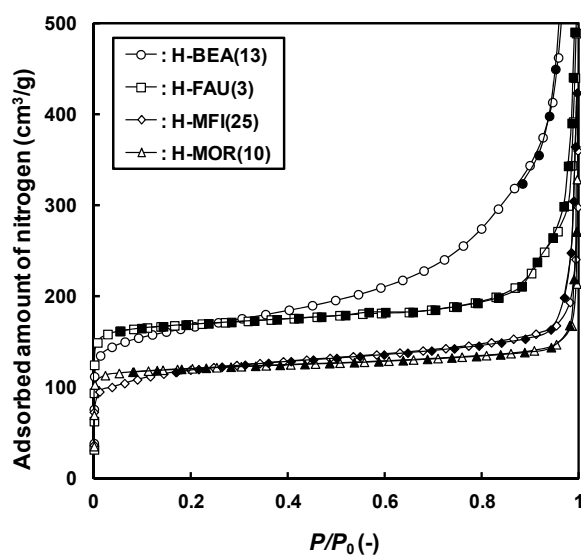


Figure 1. N₂ physisorption isotherms of the zeolite catalysts with different pore structures.

Table 1. Structural and compositional properties of the zeolites.

Zeolite	Si/Al Molar Ratio (-)	Pore Topology (MR)	Pore Size (Å)	Pore Volume (cm ³ /g)	BET Surface Area (m ² /g)	Cage Volume ^a (Å ³)
MFI	25	10	5.1 × 5.5[100] 5.3 × 5.6[010]	0.12	413	-
MOR	10	12 8	6.5 × 7.0[001] 2.6 × 5.7[001]	0.13	419	-
FAU	3	12	7.4 × 7.4[111]	0.24	589	1150
BEA	13	12	6.6 × 6.7[100] 5.6 × 5.6[001]	0.19	577	-
MWW	12	10	5.6 × 5.6[001]	0.15	420	-

^a Calculated using Marler's equation $V = \pi abc/6$ [26], where a , b and c are the pore volume and the width, length, and height of the cage, respectively. All the cages are assumed to be ideally ellipsoidal in shape.

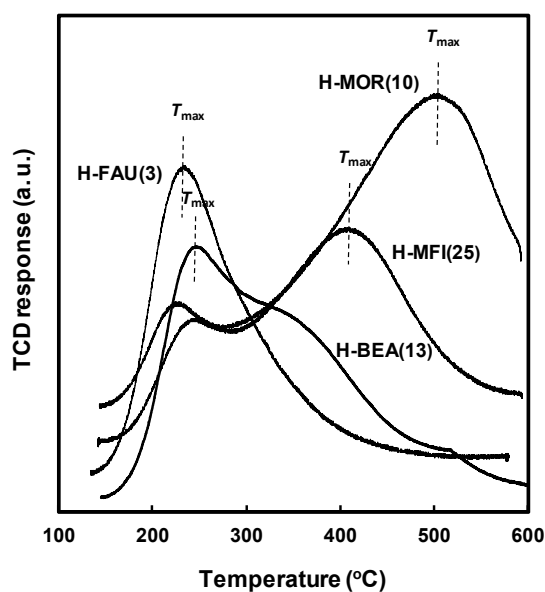


Figure 2. NH₃-TPD profiles of the zeolite catalysts.

The acid strength is estimated from the temperature of the peak maximum (T_{max}). The amount of acid sites is obtained from the area of desorption peak [28]. The T_{max} of the h -peak of the zeolites indicated that the acid strength was in the order of $FAU < BEA < MFI < MOR$. The FAU zeolite has many weak acid sites. The amount of strong acid sites is dependent on the amount of Si–O–Al bonds, whose spatial conformations can be defined by the skeletal structure of the zeolite. The T_{max} of the h -peak is the highest on the MOR zeolite, and they decreased in the order of $MFI > BEA > FAU$. This order corresponds to that of the acid strength. Figure 3 presents the NH_3 -TPD profiles of the zeolites for the various Si/Al values. As the Si/Al value increases, the acid strength measured from the T_{max} value decreases due to the increase in the number of acid sites.

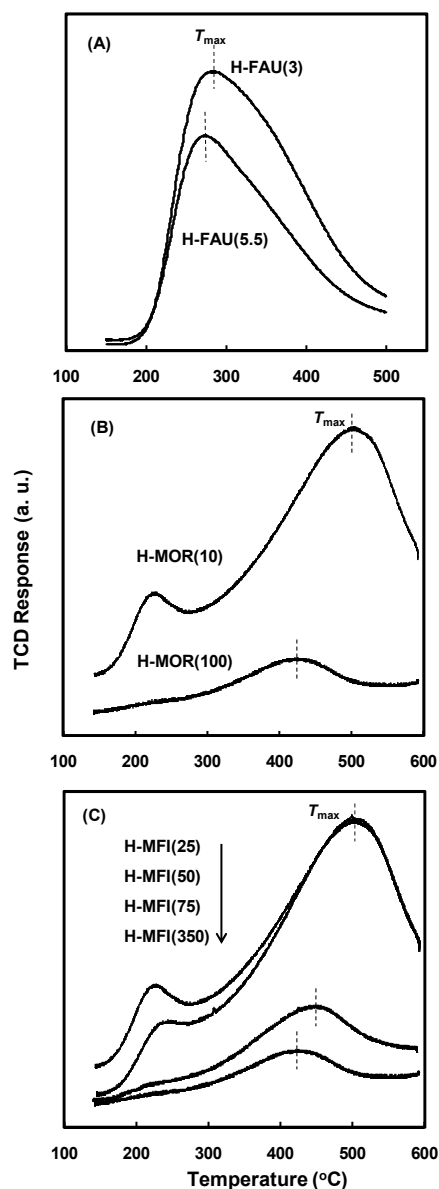


Figure 3. NH_3 -TPD profiles of H-FAU (A), H-MOR (B), and H-MFI (C) zeolite catalysts with different Si/Al molar ratios.

Figure 4 compared the IR spectra of the hydroxyl groups of the zeolites after their activation at 350 °C. The O–H stretching bands of the MFI, BEA, and MOR zeolites consisted of four kinds of O–H groups observed at about 3600, 3660, 3730, and 3780 cm^{-1} , respectively. The band at 3600 cm^{-1} arises from the O–H stretching vibration bonds in the bridging hydroxyl (acidic hydroxyl, Si–OH–Al)

groups, and those at 3660 and 3780 cm^{-1} are due to the extra framework aluminum species (EFAL, AlOH) of the non-acidic groups. The band at 3730 cm^{-1} is assigned to the O–H stretching vibration of the external silanol group ($\equiv\text{SiOH}$). On the other hand, the IR spectra of the FAU zeolites exhibited peaks at about 3560, 3600, 3631, 3660, 3730, and 3780 cm^{-1} corresponding to six kinds of OH groups. The additional bands at 3560 and 3631 cm^{-1} observed for the FAU zeolites are attributed to the acidic hydroxyl groups of the large cavities and supercages [29–31]. These spectra indicate that the concentration and strength of the acid sites differ according to the zeolite species.

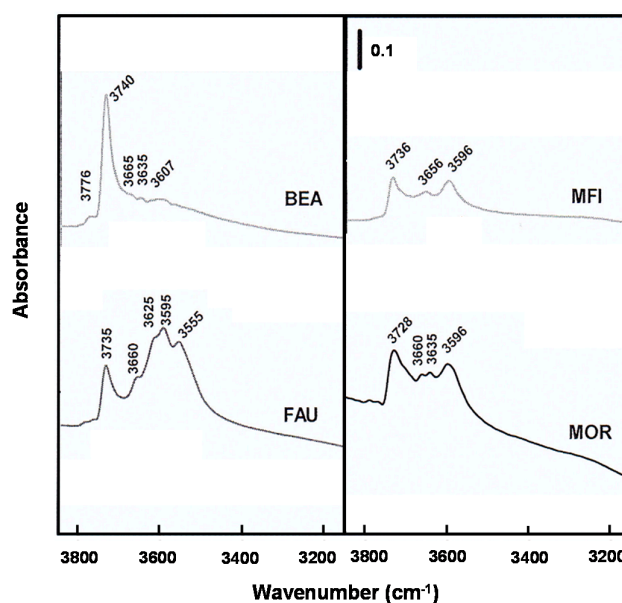


Figure 4. FT-IR spectra of the zeolites.

2.2. Catalytic Activities of the Zeolite Catalysts.

Two decyl glucosides isomers, i.e., the (α,β)-decyl glucopyranoside and (α,β)-decyl glucofuranoside isomers, were produced mainly as an anomeric mixture in this reaction. It has been noted that the glucofuranoside forms primarily, but is unstable, while the glucopyranoside forms as a stable secondary product [32,33]. A small amount of short-chain alcohols and their derivatives were also formed as byproducts through the decomposition of 1-decanol. The conversions of glucose according to the catalyst loading (catalyst/glucose mass ratio) are presented in Figure 5A. The conversions became higher with increasing catalyst loading. When the catalyst/glucose mass ratio was 0.6, the conversion exceeded 70%. However, no significant increase was observed when the catalyst loading was increased above 0.8 of catalyst/glucose mass ratio. The variations of the glucose conversion with the reaction time on the zeolite catalysts are shown in Figure 5B. The conversion increased with increasing process time and reached summit after 4 h, but it decreased after 6 h due to deactivation of the catalysts. The reaction parameters became constant when the catalyst loading was 1.0 g (catalyst/glucose mass ratio = 0.4) and the reaction temperature reached 130 °C. As shown in Figure 5B, the highest conversion was obtained on the H-FAU(3) catalyst. The sequence of the catalytic activities determined from the conversion is H-FAU > H-BEA \geq H-MFI > H-MOR. The conversion on H-MOR(10) was lower than 60%.

The variations of the yields of DGP and DGF with the reaction time are presented in Figure 6. The H-FAU(3) catalyst showed the highest yield of decyl glucosides. The yields of decyl glucosides (DGP + DGF) on the catalysts exceed 60%, except for the H-MOR(10) zeolite catalyst. The MCM-41 mesoporous materials showed a decyl glucoside yield of 60%. The yield of decyl glucoside increased slightly as reaction time increased. The isomer distribution of DGP and DGF varied according to the zeolite species.

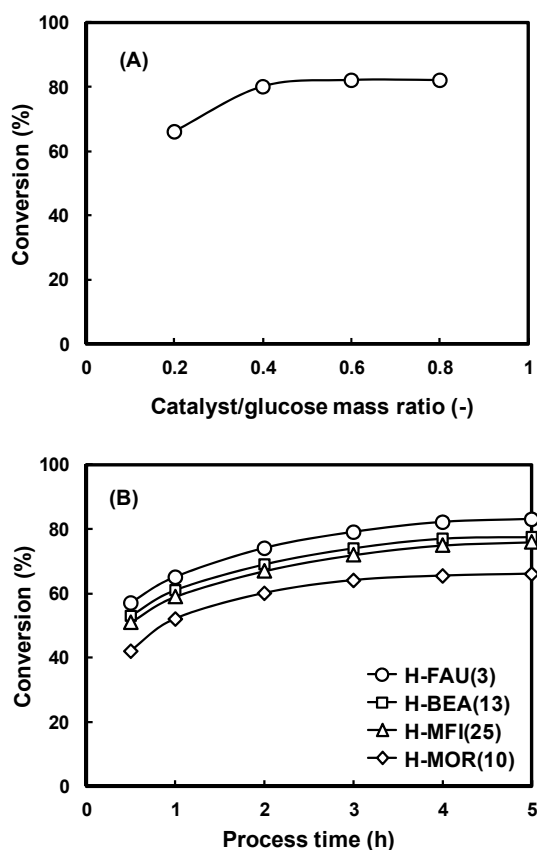


Figure 5. Variation of conversion of D-glucose with loading amount of H-MFI(50) zeolite catalyst: (A) at a process time of 4 h; and (B) variation of conversion of D-glucose with process time on various zeolite catalysts in a catalyst/glucose mass ratio of 0.6 at 130 °C.

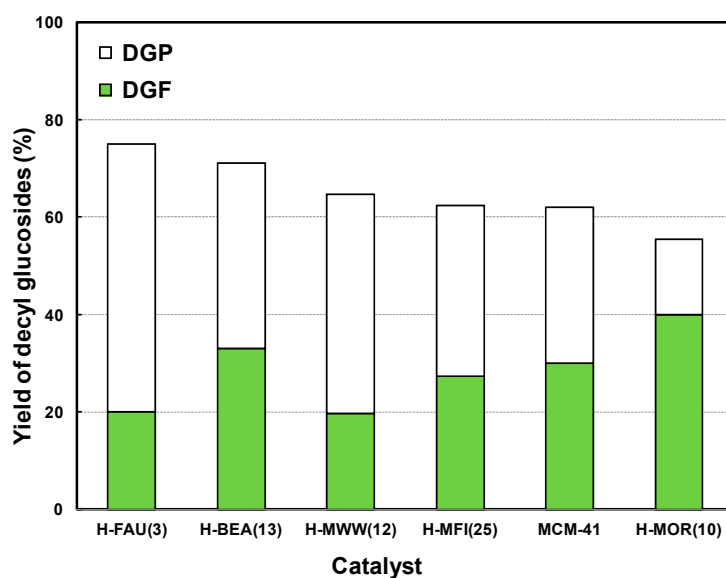


Figure 6. Yields of decyl glucosides on various zeolite catalysts at 130 °C after a process time of 4 h.

The yields of decyl glucopyranoside (DGP) and decyl glucofuranoside (DGF) on the zeolite catalysts with different Si/Al molar ratios are shown in Figure 7. The yields of decyl glucosides slightly decreased with increasing Si/Al molar ratios. The DGP yields also decreased with increasing Si/Al molar ratios to the zeolite catalysts consisting of the same pore topologies, but various amounts of acid

sites. The yield of decyl glucosides and DGP selectivity were higher over the H-FAU(3) zeolite than over the other zeolite catalysts. These results mean that weak acid site concentrations of zeolite can induce higher catalytic activity in the reaction.

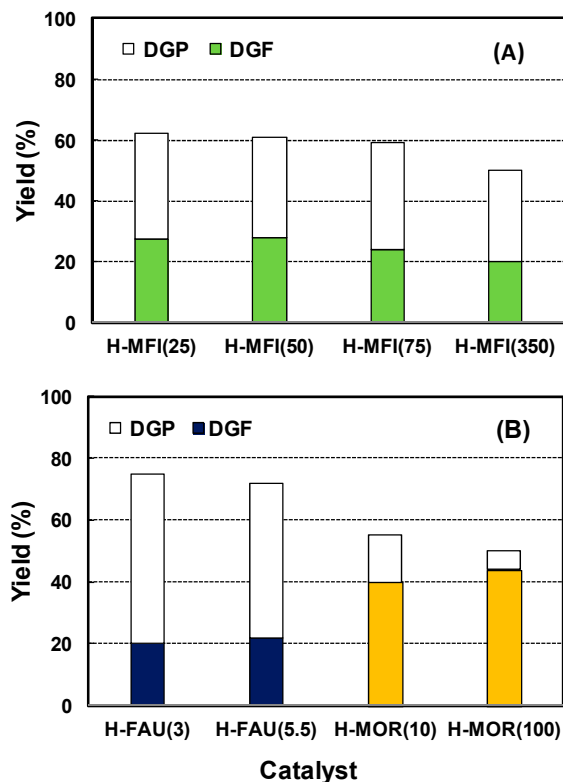


Figure 7. Yields of decyl glucosides on various zeolite catalysts with different Si/Al molar ratios in the direct glucosidation reaction catalysts at 130 °C after a process time of 4 h. (A) H-MFI zeolites, (B) H-FAU and H-MOR zeolites.

2.3. Effect of Acidic Properties of the Zeolite Catalysts

The acidic properties of the zeolite catalysts vary, and the acid strength determined from T_{max} increased in the order H/MOR > H/MFI > H/BEA \geq H/FAU, whereas their catalytic activities, i.e., conversions, decreased in this order. This indicates that the strong acid sites of the zeolites could not bring about high catalytic activities in the reaction.

The H-FAU, H-MOR, and H-MFI zeolites having various Si/Al molar ratios were examined to evaluate the influence of the number of acid sites. Because their ion exchange capacities depend on the amount of aluminum they contain, the Si/Al molar ratio indicates the amount of acid sites. Their catalytic and adsorption properties resulting from their acidity are determined by the Si/Al molar ratios of the zeolites [34]. As the ratios become higher, the amount of acid sites decreases. The acid strength becomes weaker as the Si/Al molar ratio increases, which represents a decrease in the acid site density.

The NH_3 -TPD profiles of the H-FAU, H-MOR, and H-MFI zeolites varied with the Si/Al molar ratio, as shown in Figure 3. As the Si/Al molar ratio increased, the acid strength determined from T_{max} became weaker and the concentration of acid sites was reduced. As shown in Figure 7, the yield of decyl glucosides decreased slightly with increasing Si/Al molar ratios. The DGP yield also decreased with increasing Si/Al molar ratios. The yield of decyl glucosides and DGP selectivity were higher on the H-FAU(3) zeolite than on the other zeolite catalysts. These results mean that its weak acid strength can induce high catalytic activity in the reaction.

2.4. Effect of Pore Topologies of the Zeolite Catalysts

The FAU zeolite has 12-MR tri-directional channels and super cavities in the pores. The BEA zeolite is built as 12-MR tri-directional channels without any cavities. On the contrary, MOR and MFI have narrow pore entrances as small as 10-MR. The pore channels of the MFI zeolite are composed of bidirectional zigzag channels. However, the MOR zeolite is built as a unidirectional straight channel. The pore channels of the MWW zeolite are constructed as 10- and 12-MR.

The yields of DGP and DGF exceeded 70% on the H-FAU(3) and H-BEA(13) zeolite catalysts, as shown in Figure 6, while those of the H-MWW(12), MCM-41, and H-MFI(25) zeolite catalysts were about 60%. Their high catalytic activities were derived from their weak acid sites, and the concentration of acid sites affects their activity. The yield of DGP was larger than that of DGF in the present of all the catalysts, with the exception of the H-MOR(10) catalysts. It has been reported that the selectivities of the two isomers depending on the pore structure of the zeolites are insensitive to the activation conditions [35]. The furanosides are formed from the attack of the alcohol on the glucosyl oxonium intermediate, which is a kinetically controlled reaction in the glucosidation process [36]. The more stable pyranosides are produced from them through a process of ring opening. In this process, the selectivities of the isomers are affected by the pore topologies, including the pore volume, directional pore channel, and pore cavity. This suggests that the product selectivity may be closely dependent on the pore structure which is related to the concentration of acid sites.

The H-FAU(3) catalyst showed the highest DGP selectivity of the catalysts. This is attributed to its high pore volume and numerous weak acid sites, leading the production of DGP. Its pore structure provides sufficient space volume to form pyranosides by the isomerization of the furanosides into pyranosides in the pore channels. The MCM-41 mesoporous catalyst shows relatively lower DGP selectivity compared to the H-FAU(3) catalyst. The large regular pores of the MCM-41 mesoporous catalyst admit the diffusion of reactants and conversely the fast diffusion of the products outwards [37]. It seems that its large pore channels are not able to induce sufficient secondary reaction time to form the DGP isomer, because the primary product diffuses out easily without any restriction in the pore channels.

On the contrary, the yield of DGF was higher than that of DGP on the H-MOR(10) catalyst. This suggests that the spatial restriction for the secondary reaction is insufficient to form DGP in its pore channels. This is attributed to the fact that DGF can diffuse out easily without any restriction in its pore channels, because they are built as unidirectional channels. In the H-FAU and MCM-41 catalysts, the tendencies of the product selectivities are similar, despite the differences in their pore structures. This suggests that the selectivities of the decyl glucoside isomers are dependent on the restricted transition state to the products, which in turn is affected by their pore structures and concentrations of weak acid sites.

3. Materials and Methods

3.1. Catalysts

Two kinds of FAU (zeolite Y) which have different Si/Al molar ratios ($\text{Si/Al} = 3$ and $\text{Si/Al} = 5.5$) were purchased from Zeobuilder Co. (Jeonnam, Korea). The cations of zeolites were exchanged with ammonium ions using a 2 M solution of ammonium nitrate at 80 °C. Finally, H-form zeolites were obtained by calcination at 550 °C for 24 h. The BEA (beta, Zeolyst, Conshohocken, PA, USA, $\text{Si/Al} = 13$) zeolite was also H^+ ion-exchanged using the same method. The samples were obtained through filtration, washing, and drying overnight at 120 °C after ion exchange.

The MOR (mordenite, Tosoh Co., Tokyo, Japan, $\text{Si/Al} = 10$) zeolite was employed as the parent material. To prepare the dealuminated MOR zeolites, a 6 N acetic acid (Duksan, Ansan, Korea, 99%) solution was used in the process of removing the aluminum from its framework. The parent material was treated by refluxing it in a nitric acid solution for 6 h. The dealuminated MOR zeolite was obtained through washing, drying, and calcining. The Si/Al value of the dealuminated MOR zeolite was

defined as 100. The H⁺ ion-exchanged MOR zeolites were prepared according to the ion exchange method mentioned above.

The MFI (ZSM-5) zeolites with various Si/Al values were prepared by means of a hydrothermal reaction from a synthetic mixture consisting of Ludox HS-40 colloidal silica (40 wt% SiO₂, Aldrich, St. Louis, MO, USA) potassium hydroxide (Daejung, Tokyo, Japan, 98%), aluminum hydroxide (Aldrich, St. Louis, MO, USA, 98%), and distilled water. The hydrothermal reaction of the mixture was performed through aging for 3 days and heating at 200 °C for 2 days. Their Si/Al values were 50 and 350, respectively. In addition, other MFI zeolites (Si/Al = 25 and Si/Al = 75) were purchased from Zeolyst (Tokyo, Japan). The H⁺ ion-exchanged MFI zeolites were also prepared according to the above ion exchange method.

The MWW (MCM-22) zeolite was synthesized following the method described in the literature [38] from a gel containing a hexamethyleneimine template. The crystallization of the gel was carried out in an autoclave lined with Teflon at 150 °C for 9 days under stirring. We denote the H⁺ ion-exchanged zeolites following the zeolite code names H-FAU, H-BEA, H-MFI, H-MWW, and H-MOR. Their molar ratios of Si/Al are written in parentheses after the zeolite code names.

3.2. Direct Glucosidation Reaction

Decyl glucosides were prepared from D-glucose (Sigma, St. Louis, MI, USA, 99%) with 1-decanol (Aldrich, St. Louis, MI, USA, 99%) by direct glucosidation on the zeolite catalysts. The reactor was equipped with a magnetic stirrer and a cooling system. D-glucose (2.5 g) and 1-decanol (50 mL) were introduced as the reactants. The mass of 1-decanol contained in the reactant was exceeded by about 20 times compared to the D-glucose. The anhydrous α -D-glucose and 1-decanol were put into the reactor with the zeolite catalyst. Thereafter, they were stirred together with a stirring speed of 600 rpm. To improve the glucose solubility in 1-decanol, the reactants were subjected to aging with the catalysts at 70 °C for 1 h via stirring before the reaction. After aging, the reaction was carried out directly in the reactor with stirring at 130 °C. No additional reactant was supplied during the reaction.

The compositions of the products were measured by a Younglin M600D GC (Anyang, Korea) using an HP-1 equipped capillary column with a length of 50 m and detected by an FID analyzer and GC-MS (HP-5988A, Hewlett-Packard, Avondale, PA, USA). Samples were diluted with the methanol of 5 times (volume ratio) before analyzing by GC. The components of products were confirmed by GC-MS at first. The conversion was determined as the percentage of D-glucose consumed. The decyl glucoside yields were determined as the percentage of the amount produced with respect to the sum of the total products, such as DGP and DGF. The selectivities of the decyl glucoside isomers are defined as the percentages of each isomer with respect to the sum of the isomers (DGP+DGF).

3.3. Characterization of the Zeolite Catalysts and Products

The crystallinities of the zeolites were confirmed by their XRD patterns recorded by a high-resolution X-ray powder diffractometer (XRD, Rigaku D/MAX-2500/PC, Tokyo, Japan). Ni filtered Cu K α X-ray radiation ($\lambda = 1.54056 \text{ \AA}$) was introduced. We measured the size and shape of the zeolite particles using SEM (Hitachi, S-4700, Tokyo, Japan). Their Si/Al molar ratios were confirmed with energy dispersive X-ray spectroscopy (EDS, NORAN, Z-MAX 300, Tokyo, Japan).

The N₂ physisorption isotherms of the zeolites were estimated using a volumetric adsorption apparatus (MSI, Nanoporosity-XQ, Gwangju, Korea) at liquid nitrogen temperature. The zeolites were pretreated at 200 °C for 2 h before exposing them to N₂ gas. Their BET surface areas were measured and their pore volumes were calculated using the *t*-plot [39] and BJH methods [40], respectively. Their NH₃-TPD profiles were measured using a chemisorption apparatus. The sample was evacuated in a helium gas flow at 550 °C. Thereafter, it was brought to saturation by injecting pulses of NH₃ gas at 150 °C. The ammonia adsorbed physically on the sample was purged by helium gas. The reactor was heated to 600 °C at a heating rate of 10 °C/min. The ammonia desorbed from the sample was measured using a TCD analyzer (Bel Japan, Belsorp, Osaka, Japan). The amount of acid sites was

calculated from the deconvolution of the peak from 200 °C to 700 °C. The IR spectra of the zeolites were measured with an FT-IR spectrophotometer (Bomem, MB155, Quebec, Canada). The IR spectra were obtained in the wavenumber range of 700–4000 cm⁻¹.

4. Conclusions

Decyl glucoside was synthesized by direct glucosidation reaction using zeolite catalysts that have various acidities and pore structures. The zeolite catalysts exhibited high catalytic activity in the glucosidation reaction. The highest conversion was exhibited on the H-FAU zeolite catalyst, which has a weak acid strength and many weak acid sites. The conversion and yield increased with as the number of weak acid sites increased. The catalytic activities are dependent on the amount of acid sites. The highest yield of DGP was also obtained on the H-FAU(3) catalyst. This is attributed to its high pore volume and numerous weak acid sites. The selectivities of the decyl glucoside isomers depended on the restricted transition state to the primary products due to their pore topologies. The pore structure of the H-FAU zeolite would allow sufficient spatial restriction to produce DGP by the isomerization of DGF into DGP in its broad pore channels.

Acknowledgments: This research was supported by civil research projects for solving social problems through the National Research Foundation of Korea (NRF) funded by the Ministry of Science, ICT & Future Planning (2015M3C8A6A06012988).

Author Contributions: K.C. and S.J. conceived and designed the experiments; K.C. and S.J. performed the experiments; H.P., Y.P., and K.J. analyzed the data; K.C. wrote the paper; Y.P. and S.J. revised the paper.

Conflicts of Interest: The authors declare no conflict of interest.

References

1. Scott, M.; Jones, M.N. The biodegradation of surfactants in the environment. *Biochim. Biophys. Acta* **2000**, *1508*, 235–251. [[CrossRef](#)]
2. Soares, A.; Guieysse, B.; Jefferson, B.; Cartmell, E.; Lester, J. Nonylphenol in the environment: A critical review on occurrence, fate, toxicity and treatment in wastewaters. *Environ. Int.* **2008**, *34*, 1033–1049. [[CrossRef](#)] [[PubMed](#)]
3. Dodds, E.C.; Lawson, W. Molecular structure in relation to oestrogenic activity. Compounds without a phenanthrene nucleus. *Proc. R. Soc. Lond. B* **1938**, *125*, 222–232. [[CrossRef](#)]
4. Soto, A.M.; Justicia, H.; Wray, J.; Sonnenschein, C. *p*-Nonyl-phenol: An estrogenic xenobiotic released from “modified” polystyrene. *Environ. Health Perspect.* **1991**, *92*, 167–173. [[CrossRef](#)] [[PubMed](#)]
5. Lee, H.J.; Chattopadhyay, S.; Gong, E.Y.; Ahn, R.S.; Lee, K. Antiandrogenic effects of bisphenol A and nonylphenol on the function of androgen receptor. *Toxicol. Sci.* **2003**, *75*, 40–46. [[CrossRef](#)] [[PubMed](#)]
6. De Nijs, P.M.; Maat, L.; Kieboom, A.P.G. Two-step chemo-enzymatic synthesis of octyl 6-O-acyl- α -D-glucopyranoside surfactants from glucose. *Recl. Trav. Chim. Pays-Bas* **1990**, *109*, 429–433. [[CrossRef](#)]
7. Lee, S.M.; Lee, J.Y.; Yu, H.P.; Lim, J.C. Synthesis of environment friendly nonionic surfactants from sugar base and characterization of interfacial properties for detergent application. *J. Ind. Eng. Chem.* **2016**, *38*, 157–166. [[CrossRef](#)]
8. Ferlin, N.; Duchet, L.; Kovensky, J.; Grand, E. Microwave-assisted synthesis of long-chain alkyl glucopyranosides. *Carbohydr. Res.* **2008**, *343*, 2819–2821. [[CrossRef](#)] [[PubMed](#)]
9. Hill, K.; von Rybinski, W.; Stoll, G. *Alkyl Polyglucosides: Technology, Properties and Applications*; VCH: Weinheim, Germany, 1997.
10. Hurford, J.R.; Lee, C.K. *Developments in Food Carbohydrate 2*; Lee, C.K., Ed.; Applied Science Publishers Ltd.: London, UK, 1980; pp. 327–350.
11. Hughes, F.A.; Lew, B.W.; Am, J. Physical and functional properties of some higher alkyl polyglucosides. *Chem. Soc.* **1970**, *47*, 162–167. [[CrossRef](#)]
12. Straathof, A.J.J.; van Bekkum, H.; Kieboom, A.P.G. Efficient preparation of octyl α -D-glucopyranoside monohydrate: A recirculation procedure involving water removal by product crystallization. *Starch-Stärke* **1998**, *40*, 229–234. [[CrossRef](#)]

13. Le Coz, C.J.; Meyer, M.T. Contact allergy to decyl glucoside in antiseptic after body piercing. *Contact Dermat.* **2003**, *48*, 279–280. [[CrossRef](#)]
14. Andersen, K.E.; Goossens, A. Decyl glucoside contact allergy from a sunscreen product. *Contact Dermat.* **2006**, *54*, 349–350. [[CrossRef](#)] [[PubMed](#)]
15. Andrade, P.; Goncalo, M.; Figueiredo, A. Allergic contact dermatitis to decyl glucoside in Tinosorb M[®]. *Contact Dermat.* **2010**, *62*, 119–120. [[CrossRef](#)] [[PubMed](#)]
16. Blondeel, A. Contact allergy to the mild surfactant decylglucoside. *Contact Dermat.* **2004**, *49*, 304–305. [[CrossRef](#)] [[PubMed](#)]
17. Horn, H.M.; Murray, C.; Aldridge, R.D. Contact allergy to decyl glucoside. *Contact Dermat.* **2005**, *52*, 227–228. [[CrossRef](#)] [[PubMed](#)]
18. Krehic, M.; Avenel-Audran, M. Allergic contact dermatitis from decyl glucoside in an antiseptic lotion. *Contact Dermat.* **2009**, *61*, 349–350. [[CrossRef](#)] [[PubMed](#)]
19. Ludot, C.; Estrine, B.; Le Bras, J.; Hoffmann, N.; Marinkovic, S.; Muzart, J. Sulfoxides and sulfones as solvents for the manufacture or alkyl polyglycosides without added catalyst. *Green Chem.* **2013**, *15*, 3027–3030. [[CrossRef](#)]
20. Van Es, D.S.; Marinkovic, S.; Oduber, X.; Estrine, B. Use of furandicarboxylic acid and its decyl ester as additives in the Fischer's glycosylation of decanol by D-glucose: Physicochemical properties of the surfactant compositions obtained. *J. Surfactant Deterg.* **2013**, *16*, 147–154. [[CrossRef](#)]
21. McCurry, P.M., Jr.; Pickens, C.E. Process for Preparation of Alkylglycosides. U.S. Patent 4,950,743, 21 August 1990.
22. Mazumder, N.A.; Rano, R.; Sarmah, G. A green and efficient solid acid catalyst from coal fly ash for Fischer esterification reaction. *J. Ind. Eng. Chem.* **2015**, *32*, 211–217. [[CrossRef](#)]
23. Boettner, F.E. Alkylpolyalkoxyalkyl Glucosides and Process of Preparation Therefor. U.S. Patent 3,219,656, 23 November 1965.
24. Corma, A.; Iborra, S.; Miquel, S.; Primo, J. Preparation of long-chain alkyl glucoside surfactants by one-step direct Fischer glucosidation, and by transacetalation of butyl glucosides on beta zeolite catalysts. *J. Catal.* **1998**, *180*, 218–224. [[CrossRef](#)]
25. Robeson, H.; Lillerud, K.P. *Verified Syntheses of Zeolitic Materials*, 2nd ed.; Elsevier: Amsterdam, The Netherlands, 2001; pp. 225–227.
26. Cerqueira, H.S.; Ayrault, P.; Darka, J.; Magnoux, P.; Guisnet, M. Influence of coke on the acid properties of a USHY zeolite. *Micropor. Mesoporous Mater.* **2000**, *38*, 197–205. [[CrossRef](#)]
27. Kadata, N.; Igi, H.; Kim, J.-H.; Niwa, M. Determination of the acidic properties of zeolite by theoretical analysis of temperature-programmed desorption of ammonia based on adsorption equilibrium. *J. Phys. Chem. B* **1997**, *101*, 5969–5977. [[CrossRef](#)]
28. Niwa, M.; Kadata, N.; Sawa, M.; Murakami, Y. Temperature-programmed desorption of ammonia with readsorption based on the derived theoretical equation. *J. Phys. Chem. B* **1995**, *99*, 8812–8816. [[CrossRef](#)]
29. Marques, J.P.; Gener, I.; Ayrault, P.; Bordado, J.C.; Lopes, J.M.; Ribeiro, F.R.; Guisnet, M. Dealumination of HBEA zeolite by steaming and acid leaching: Distribution of the various aluminic species and identification of the hydroxyl groups. *R. C. Chim.* **2005**, *8*, 399–410. [[CrossRef](#)]
30. Cerqueira, H.S.; Ayrault, P.; Datka, J.; Magnoux, P.; Guisnet, M. *m*-Xylene transformation over a USHY zeolite at 523 and 723 K: Influence of coked deposits on activity, acidity and porosity. *J. Catal.* **2000**, *196*, 149–157. [[CrossRef](#)]
31. Kotrel, S.; Rosynek, M.P.; Lunsford, J.H. Quantification of acid sites in H-ZSM-5, H- β , and H-Y Zeolites. *J. Catal.* **1999**, *182*, 278–281. [[CrossRef](#)]
32. Miyamoto, Y.; Katada, N.; Niwa, M. Acidity of β zeolite with different Si/Al₂ ratio as measured by temperature programmed desorption of ammonia. *Micropor. Mesoporous Mater.* **2000**, *40*, 271–281. [[CrossRef](#)]
33. Lonyi, F.; Valyon, J. On the interpretation of the NH₃-TPD patterns of H-ZSM-5 and H-mordenite. *Micropor. Mesoporous Mater.* **2001**, *47*, 293–301. [[CrossRef](#)]
34. Bennet, A.J.; Sinnott, M.L.; Wijesundera, W.S. ¹⁸O and secondary ²H kinetic isotope effects confirm the existence of two pathways for acid-catalyzed hydrolyses of α -arabinofuranosides. *J. Chem. Soc. Perkin Trans.* **1985**, *2*, 1233–1236. [[CrossRef](#)]
35. Farris, D.D. Process for preparation of alkyl glycosides. European Patent 0096917, 28 December 1983.

36. Thiem, J.; Böcker, T. Alkyl glycoside surfactants-synthesis and properties. *Spec. Publ. R. Soc. Chem.* **1992**, *107*, 123–147.
37. Weitkamp, J.; Hunger, M. Acid and base catalysis on zeolites. In *Studies in Surface Science and Catalysis*; Cejka, J., van Bekkum, H., Corma, A., Schuth, F., Eds.; Elsevier: Amsterdam, The Netherlands, 2007; Chapter 22.
38. Yue, C.; Xie, W.; Liu, Y.; Wu, H.; Li, X.; Wu, P. Hydrothermal synthesis of MWW-type analogues using linear-type quaternary alkylammonium hydroxides as structure-directing agents. *Micropor. Mesoporous Mater.* **2011**, *142*, 347–353. [[CrossRef](#)]
39. Sing, K.S.W.; Williams, R.T. Physisorption hysteresis loops and the characterization of nanoporous materials. *Adsorpt. Sci. Technol.* **2004**, *22*, 773–782. [[CrossRef](#)]
40. Barrett, E.P.; Joyner, L.G.; Halenda, P.P. The determination of pore volume and area distributions in porous substances. I. Computations from nitrogen isotherms. *J. Am. Chem. Soc.* **1951**, *73*, 373–380. [[CrossRef](#)]



© 2016 by the authors; licensee MDPI, Basel, Switzerland. This article is an open access article distributed under the terms and conditions of the Creative Commons Attribution (CC-BY) license (<http://creativecommons.org/licenses/by/4.0/>).